EGU2016-5332

# A data-derived forecast model of surface circulation based on statistical forcing-response decomposition technique


Sung Yong Kim†

[1]Department of Mechanical Engineering, Korea Advanced Institute of Science and Technology, Republic of Korea

†syongkim@kaist.ac.kr



## Abstract

This paper presents a data-derived surface current forecast model based on statistical decomposition techniques [[1]] on the observations of high-frequency radar-derived surface currents, local winds, and sea surface height anomalies (SSHA) off southern San Diego. The regional surface circulation mainly consists of tide-, wind-, and low-frequency pressure gradient-coherent components, and residual currents, which leads us to use tidal harmonic analysis, response functions using wind stress and pressure gradients, autoregressive analysis, respectively, in the forecast model. These basis functions have been consecutively added, and the performance of corresponding forecast models is evaluated.


## Introduction

As one of geophysical boundary flows at the air-sea-land interface, coastal circulation is associated with complex responses to a combination of geophysical forces of tides, wind stress, heat flux, and low-frequency forcing and their interactions [e.g., [2, 3, 4, 5]]. Understanding of ocean physics and bio-geo-chemistry, and their interactions in coastal regions has been addressed with in-situ observations, numerical simulations, and theories such as environmental sensing and data analysis, computational fluid dynamics, and theoretical studies on geophysical fluid dynamics, respectively. Particularly, coastal dynamics is vital for tracking of water-borne materials (e.g., search and rescue, oil spill, and larvae) and for studying of coastal processes, beach erosion, sea level rise, and fishery science [e.g., [6]; add more].

In the awareness of importance of ocean physics and biogeochemistry, the forecasting skill and models have been developed with regional numerical models and concurrent in-situ observations along with data assimilation techniques [refs]. Among them, the statistical and dynamical data analyses have elucidated the coastal ocean dynamics [[5, 1]]. [7] proposed a stochastic forecast model based on harmonic analysis for tide-coherent surface currents and autoregressive process (e.g., Gauss-Markov method) for residual surface currents in order to derive surface trajectory for search and rescue missions. Primary distinction of this paper is to present a near-real time forecast model based on observations of surface currents, tide gauges, along-track altimeter, and local wind data by accumulating them as regression basis functions and evaluate performance of the forecast model in terms of individual basis functions.

# Data Analysis

## Data

### Surface currents

Hourly surface current maps off southern San Diego are obtained from an array of three high-frequency radars for a period of three years (2007 to 2009). Data for a period of the first two years are used for training a model and the rest of data is used for forecasting. The statistical decomposition of surface currents are reported elsewhere [[1]].

### Sea surface heights

The sea surface elevations at tide gauges in San Diego Bay and Los Angeles are analyzed to derive along-shore geostrophy-coherent components. Moreover, along-track and optimally interpolated sea surface height anomalies obtained from AVISO around southen San Diego are used to estimate the pressure gradients in the cross-shore and along-shore directions.

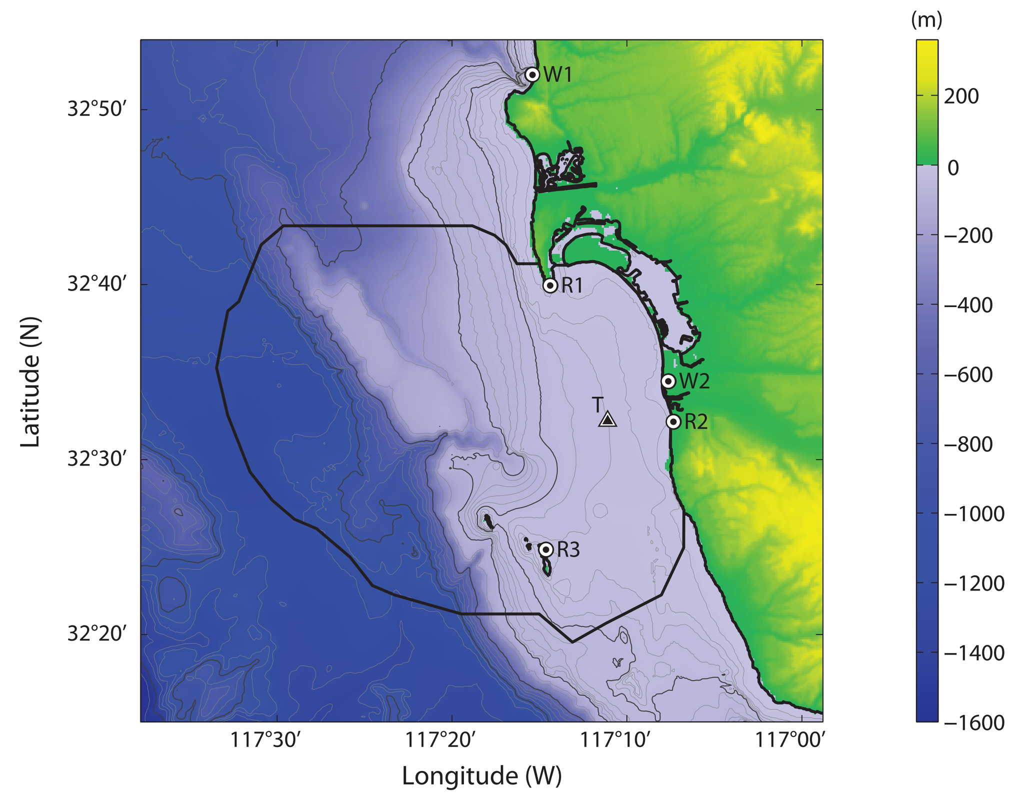


Figure 1: An observation domain of submesoscale eddies using in-situ observations: Three HF radars [R1 (Point Loma), R2 (Imperial Beach), and R3 (Coronado Islands)] for surface currents, two stations at the Scripps Pier (W1, SIO) and Tijuana River Valley (W2, TJR) for wind, and one mooring (T) for both subsurface currents (ADCP) and temperature profile. A black outline denotes the effective coverage area of HF radars (at least 70% data availability for two years). The bottom bathymetry contours are indicated by thin curves with 10 m ($0 < z < 100$ m) and 50 m ($100 < z < 1000$ m) contour intervals and thick curves at the 50, 100, 500, and 1000 m depths.

### Coastal winds

The wind observations at Scripps Pier, Tijuana River, and NDBC buoy (46086) are used to derived wind response functions [e.g., [8]].

## Hindcast analysis

The archived surface currents can be decomposed into tide-coherent (barotropic or baroclinic tides, or both), wind-coherent, primary-frequency-band. geostrophy-coherent, and residual components using harmonic analysis, slow-FFT analysis, wind- and sea-level-response functions, and auto-regressive model, respectively [e.g., [1]]:

$$\mathbf{u}(t) = \langle \mathbf{u}(t) \rangle + \mathbf{u}_T(t) + \mathbf{u}_W(t) + \mathbf{u}_S(t) + \mathbf{u}_G(t) + \mathbf{u}_R(t), \tag{1}$$

where $\mathbf{u}_T$, $\mathbf{u}_W$, $\mathbf{u}_S$, $\mathbf{u}_G$, and $\mathbf{u}_R$ denote tide-coherent, wind-coherent, primary-frequency-band, geostrophy-coherent, and residual surface currents, respectively. The time mean, $\langle \mathbf{u}(t) \rangle$, is removed prior to the harmonic analysis and updated during regression [see [9] for more details].

### Harmonic analysis

For the primary tidal constituents and unique resonance frequencies due to bay and harbor effects, the tidal surface currents are isolated:

$$\mathbf{u}_T(t) = \sum_{k=1}^{K} A_k \cos\sigma_k t + B_k \sin\sigma_k t, \tag{2}$$

where

$$\hat{\mathbf{m}} = \left(\mathbf{G}\mathbf{G}^\dagger\right)^{-1} \mathbf{G}^\dagger \mathbf{u} \tag{3}$$

and $\hat{\mathbf{m}} = [A_k \;\; B_k]^\dagger$ and $\mathbf{G} = [\cos\sigma_1 t \; \cdots \; \cos\sigma_k t \;\; \sin\sigma_1 t \; \cdots \sin\sigma_k t]^\dagger$.

### Auto-regressive model

The auto-regressive model is applied to residual surface currents ($\mathbf{u}_{R_{\{\cdot\}}}$) by regressing time-lagged basis functions:

$$\mathbf{u}_R(t) = \sum_{l=1}^{L} C_l \mathbf{u}_R(t - l\Delta t), \tag{4}$$

where

$$C_l = \frac{\langle \mathbf{u}_R(t)\mathbf{u}_{R,L}^\dagger(t) \rangle}{\langle \mathbf{u}_{R,L}(t)\mathbf{u}_{R,L}^\dagger(t) \rangle + \langle \boldsymbol{\epsilon}_C \boldsymbol{\epsilon}_C^\dagger \rangle}, \tag{5}$$

$\mathbf{u}_{R,L}(t)$ denotes the $L$ time lagged of residual currents, $\mathbf{u}_R(t)$ (two subscripts separated by comma indicate the decomposed components and the number time lags), and $\boldsymbol{\epsilon}_{\{\cdot\}}$ indicates the noise level of impulses (e.g., $\mathbf{u}_{R,L}$, $\boldsymbol{\tau}_M$, and $\mathbf{u}_{S,L}$ in equations below) to constitute the regularization matrix ($\langle \boldsymbol{\epsilon}_{\{\cdot\}} \boldsymbol{\epsilon}_{\{\cdot\}} \rangle$).

### Wind response function

The tidal-residual surface currents are decomposed with the wind response function and auto-regressive model:

$$\mathbf{u}_W(t) = \sum_{m=1}^{M} D_m \boldsymbol{\tau}(t - m\Delta t), \tag{6}$$

where

$$D_m = \frac{\langle \mathbf{u}(t)\boldsymbol{\tau}_M^\dagger(t) \rangle}{\langle \boldsymbol{\tau}_M(t)\boldsymbol{\tau}_M^\dagger(t) \rangle + \langle \boldsymbol{\epsilon}_D \boldsymbol{\epsilon}_D^\dagger \rangle}, \tag{7}$$

(8)

and $\boldsymbol{\tau}_M(t)$ denotes the $M$ time lagged $\boldsymbol{\tau}(t)$.

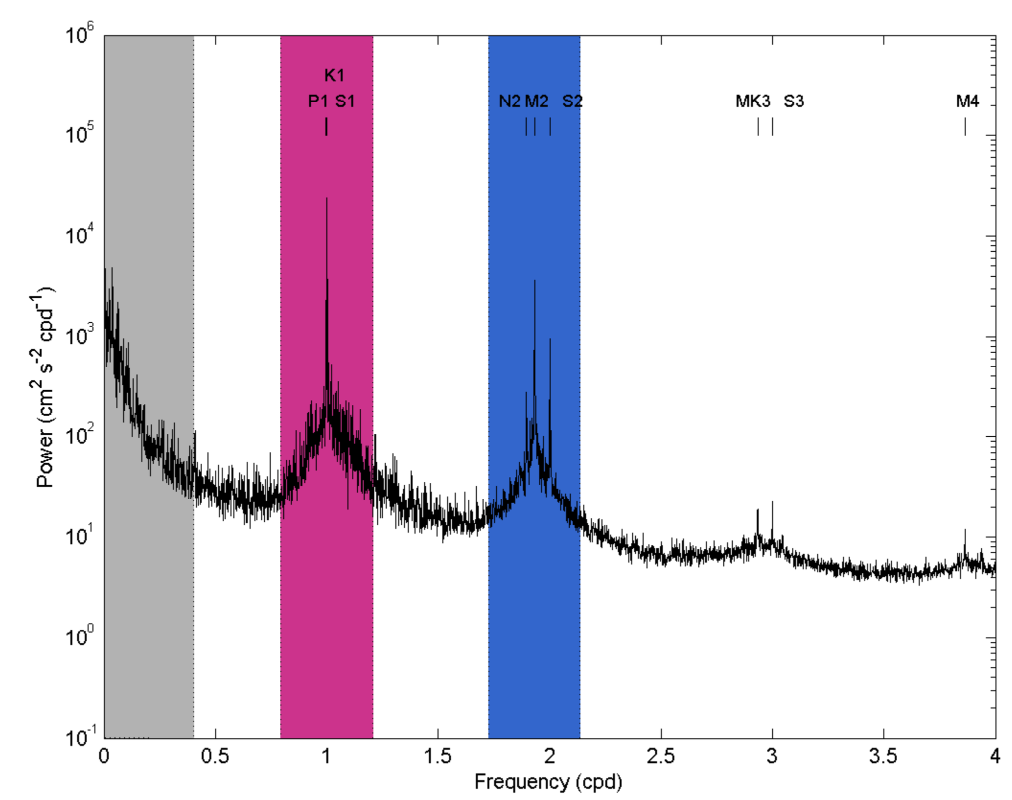


Figure 2: Regionally averaged power spectrum of hourly surface vector currents in the region with 45% or greater coverage (1337 grid points) shows that the dominant variances are at the low frequencies (less than 0.4 cpd), and the main tidal frequencies (K1 and M2) and their harmonics.

### Slow-FFT analysis

For the primary frequency bands (e.g., diurnal, semi-diurnal, and low-frequency), the slow-FFT analysis is applied to isolate relevant variance:

$$\mathbf{u}_S(t) = \sum_{n=1}^{N} E_n \cos\sigma_n t + F_n \sin\sigma_n t, \tag{9}$$

where

$$\hat{\mathbf{m}} = \left(\mathbf{G}\mathbf{G}^\dagger + \alpha^2 \mathbf{I}\right)^{-1} \mathbf{G}^\dagger \mathbf{u} \tag{10}$$

and $\hat{\mathbf{m}} = [E_n \;\; F_n]^\dagger$ and $\mathbf{G} = [\cos\sigma_1 t \; \cdots \; \cos\sigma_n t \;\; \sin\sigma_1 t \; \cdots \sin\sigma_n t]^\dagger$. $\alpha^2$ is the regularization coefficient to control the variance associated with regression between overfitting and underfitting.

### Geostrophic response function

The detided sea surface elevations at local tide gauges or altimeters can be used as the basis function.

$$\mathbf{u}_G(t) = \sum_{p=1}^{P} -H_p \frac{g}{f_c} \nabla \left[\eta_{\parallel}(t - p\Delta t)\mathbf{k}\right], \tag{11}$$

where

$$H_p = \frac{\langle \mathbf{u}_G(t)\eta^\dagger(t) \rangle}{\langle \eta(t)\eta^\dagger(t) \rangle + \langle \boldsymbol{\epsilon}_H \boldsymbol{\epsilon}_H^\dagger \rangle}. \tag{12}$$

$\mathbf{u}_G$ denotes the cross-track geostrophic currents.

## Forecast analysis

The hindcast analysis derives forcing-response relationships using the training data ($\mathbf{u}_{TR}$) for a period of two years, and the forecast analysis is executed to add decomposed components consecutively and to evaluate the performance by comparing the forecast data ($\mathbf{u}_{FR}$) and testing data ($\mathbf{u}_{TS}$) .

$$\kappa = 1 - \frac{\langle (\mathbf{u}_{TS} - \mathbf{u}_{FR})^2 \rangle}{\langle \mathbf{u}_{TS}^2 \rangle} \tag{13}$$

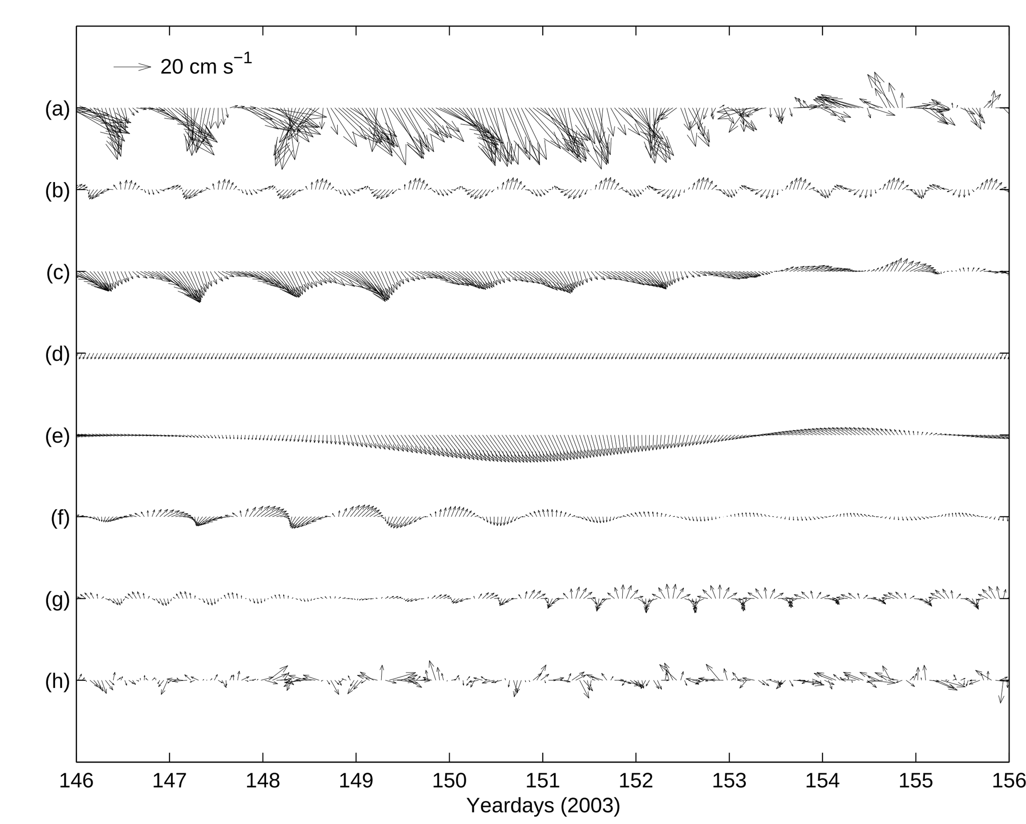


Figure 3: An example of a set of time series of decomposed surface currents at the location T in Figure 1. (a) Unconditioned surface currents ($\mathbf{u}$). (b) Surface currents driven by pure tides ($\mathbf{u}_t$). (c) Locally wind-driven surface currents ($\mathbf{u}_w$). (d) Mean surface currents ($\langle \mathbf{u} \rangle$). (e) Surface currents in the low frequency band ($\mathbf{u}_L$). (f) Surface currents in the frequency band centered on diurnal frequency ($\mathbf{u}_D$). (g) Surface currents in the frequency band centered on semidiurnal frequency ($\mathbf{u}_S$). (h) Residual surface currents ($\mathbf{u}_r$).

Table 1: The variance fraction (%) of the decomposed surface currents. The variance of surface currents coherent with alongshore pressure difference is approximately 3% of total variance.

| Pure tide | Wind | Mean | Low | Diurnal | Semidiurnal | Residual |
|---|---|---|---|---|---|---|
| 6.3 | 32.6 | 1.4 | 31.8 | 8.9 | 4.1 | 14.9 |

# Conclusion

A data-derived surface current forecast model is formulated based on statistical decomposition techniques on the observations of high-frequency radar-derived surface currents, local winds, and sea surface height anomalies off southern San Diego. Considering the primary components in the regional surface circulation – tide-, wind-, and low-frequency pressure gradient-coherent components, and residual currents, we adopt the tidal harmonic analysis, response functions using wind stress and pressure gradients, and autoregressive analysis. respectively, in the forecast model.


### Acknowledgement

Sung Yong Kim is supported by the Basic Science Research Program through the National Research Foundation (NRF), Ministry of Education (NRF-2013R1A1A2057849), the Human Resources Development of the Korea Institute of Energy Technology Evaluation and Planning (KETEP), Ministry of Trade, Industry and Energy (no. 20134030200300), Republic of Korea. Surface current data are provided from the Southern California Coastal Ocean Observing System (SCCOOS, Available online at `http://www.sccoos.org`) at Scripps Institution of Oceanography (SIO). Wind data at the Tijuana River (Tidal Linkage) are maintained by the System.Wide Monitoring Program at the Tijuana River National Estuarine Research Reserve, Estuarine Reserves Division (TRNERR), NOAA, Centralized Data Management Office (CDMO), Baruch Marine Field Lab, and University of South Carolina. Wind data at the SIO Pier are maintained by the Integrative Oceanography Division (IOD).


# References


[1] S. Y. Kim, B. D. Cornuelle, and E. J. Terrill. Decomposing observations of high-frequency radar derived surface currents by their forcing mechanisms: Decomposition techniques and spatial structures of decomposed surface currents. *J. Geophys. Res.*, 115, 2010.

[2] C. D. Winant. Coastal circulation and wind-induced currents. *Annu. Rev. Fluid Mech.*, 12:271–301, 1980.

[3] J. S. Allen. Models of wind-driven currents on the continental shelf. *Annu. Rev. Fluid Mech.*, 12:389–433, 1980.

[4] K. H. Brink. Coastal-trapped waves and wind-driven currents over the continental shelf. *Annu. Rev. Fluid Mech.*, 23:389–412, 1991.

[5] S.J. Lentz and M.R. Fewings. The wind-and wave-driven inner-shelf circulation. *Annu. Rev. Mar. Sci.*, pages 317–343, 2012.

[6] S. Y. Kim, E. J. Terrill, and B. D. Cornuelle. Assessing coastal plumes in a region of multiple discharges: the U.S.–Mexico border. *Environ. Sci. Technol.*, 43(19):7450–7457, 2009.

[7] D. S. Ullman, J. O'Donnell, J. Kohut, T. Fake, and A. Allen. Trajectory prediction using HF radar surface currents: Monte Carlo simulations of prediction uncertainties. *J. Geophys. Res.*, 111, 2006.

[8] S. Y. Kim, B. D. Cornuelle, and E. J. Terrill. Decomposing observations of high-frequency radar derived surface currents by their forcing mechanisms: Locally wind-driven surface currents. *J. Geophys. Res.*, 115, 2010.

[9] S. Y. Kim and B. D. Cornuelle. Coastal ocean climatology of temperature and salinity off the Southern California Bight: Seasonal variability, climate index correlation, and linear trend. *Prog. Oceanogr.*, 138:136 – 157, 2015.